

IMAGING DIAGNOSIS—SPINAL CORD HISTIOCYTIC SARCOMA IN A DOG

AMANDA TAYLOR, BUNITA EICHELBERGER, CAROLYN HODO, JOCELYN COOPER, BRIAN PORTER

A 12-year-old mixed breed dog was presented for evaluation of progressive paraparesis and ataxia. Magnetic resonance (MR) imaging was performed and identified multifocal intradural spinal cord mass lesions. The lesions were hyperintense in T2-weighted sequences, isointense to mildly hyperintense in T1-weighted sequences with strong contrast enhancement of the intradural lesions and spinal cord meninges. Spinal cord neoplasia was suspected. A diagnosis of intramedullary spinal cord histiocytic sarcoma, confined to the central nervous system, was confirmed histopathologically. Spinal cord histiocytic sarcoma is a rare neoplasm, but should be included in the differential diagnosis for dogs with clinical signs of myelopathy. © 2014 American College of Veterinary Radiology.

Key words: central nervous system, histiocytic sarcoma, MRI, neoplasia, spinal cord.

Signalment, History, and Clinical Findings

A 12-YEAR-OLD NEUTERED MALE mixed breed dog was presented to the Texas A&M University Small Animal Veterinary Medical Teaching Hospital for a one week history of progressive left pelvic limb monoplegia and right pelvic limb paresis. Voluntary motor function and superficial pain perception were absent in the left pelvic limb, but deep pain perception was present. Segmental spinal reflexes were normal bilaterally. The cutaneous trunci reflex cutoff was at the level of T8–T9 on the left and T11 on the right. No paraspinal hyperesthesia was appreciated. Neuroanatomical localization was to the T3–L3 spinal cord segments. The clinically significant neurologic findings were the neuroanatomical localization and pelvic limb pain and motor deficits. Additional diagnostic testing revealed no concurrent systemic disease processes. Cerebrospinal fluid (CSF) was collected from the cisterna magna (lumbar collection was attempted but was unsuccessful) and was unremarkable. Magnetic resonance imaging was pursued to determine the cause of the clinical signs.

Imaging, Diagnosis, and Outcome

Magnetic resonance (MR) images were acquired with a 3.0 Tesla scanner (Siemens Verio, Siemens, Malvern, PA).

From the Small Animal Clinical Sciences, (Taylor), Large Animal Clinical Sciences (Eichelberger), and Pathobiology (Hodo, Porter), Veterinary Medicine and Biomedical Sciences, Texas A&M University, College Station, TX 77843 and Mission Veterinary Specialists, San Antonio, TX 78249 (Cooper).

Address correspondence and reprint requests to Bunita Eichelberger, at the above address. E-mail: BEichelberger@cvm.tamu.edu

Received June 12, 2013; accepted for publication October 20, 2013.
doi: 10.1111/vru.12135

Sequences acquired for imaging were: Sagittal half-Fourier acquisition single-shot turbo spin-echo (HASTE) (TR 1250.0 ms, TE 226.0 ms, 2.0 mm); T1-weighted (TR 871.0–1270.0 ms, TE 11.0–18.0 ms, and 2.0–3.0 mm) and T2-weighted (TR 3440.0–8420.0 ms, TE 105.0–114.0 ms, and 2.0–3.0 mm) turbo spin-echo in the sagittal and transverse planes; dorsal and transverse short tau inversion recovery (STIR) (4000.0–5112.8 ms, TE 34.0–40.0 ms, 2.0–3.0 mm); and transverse T2-weighted with chemical fat suppression (FATSAT) (TR 5000.0 ms, TE 79.0 ms, 3.0 mm). Postcontrast sagittal, transverse, and dorsal T1-weighted with chemical FATSAT sequences (625.0–844.0 ms, 9.2–11.0 ms, 2.0–3.0 mm) were obtained after IV administration of gadolinium (Magnevist™ Bayer HealthCare, Wayne NJ).

The sagittal HASTE sequence showed a signal void consistent with magnetic susceptibility and obstruction to cerebral spinal fluid flow from the level of the T8 through T10 vertebral bodies. T2- and T1-weighted images demonstrated generalized enlargement of the spinal cord from T8–T11 as evidenced by the loss of the subarachnoid space and epidural fat signal. On transverse T2-weighted and STIR sequences, there was generalized hyperintensity of the spinal cord parenchyma equal to the length of the T8 vertebral body, with a focal, sharply demarcated right-sided intramedullary mass at the level of T9. The mass was hyperintense compared to spinal cord parenchyma with a more hyperintense rim on T2-weighted images. Just caudal to the right-sided mass, there was a separate sharply demarcated left-sided intramedullary mass with similar imaging characteristics that effaced approximately 75% of the spinal cord parenchyma (Fig. 1C). There was mild dilation of the central canal cranial and caudal to the described mass lesions.

Vet Radiol Ultrasound, Vol. 56, No. 2, 2015, pp E17–E20.

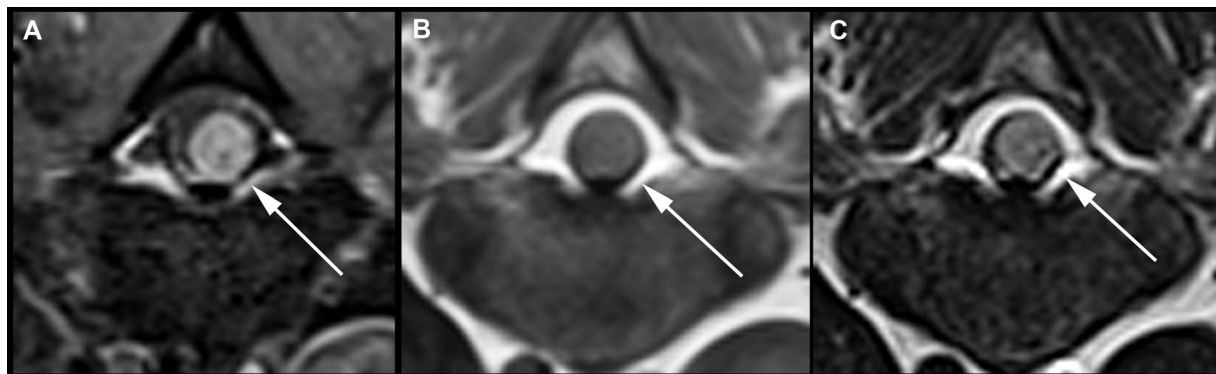


FIG. 1. (A) Transverse T1-weighted image with chemical fat suppression postcontrast administration (TR 844.0 ms, TE 9.2 ms, and 3.0 mm). (B) Transverse T1-weighted image (TR 871.0 ms, TE 18.0 ms, and 3.0 mm). (C) Transverse T2-weighted image (TR 8420.0 ms, TE 107.0 ms, and 3.0 mm). The lesion is uniformly T2 hyperintense and T1 isointense to hyperintense. The lesion uniformly and strongly contrast enhances postcontrast administration.

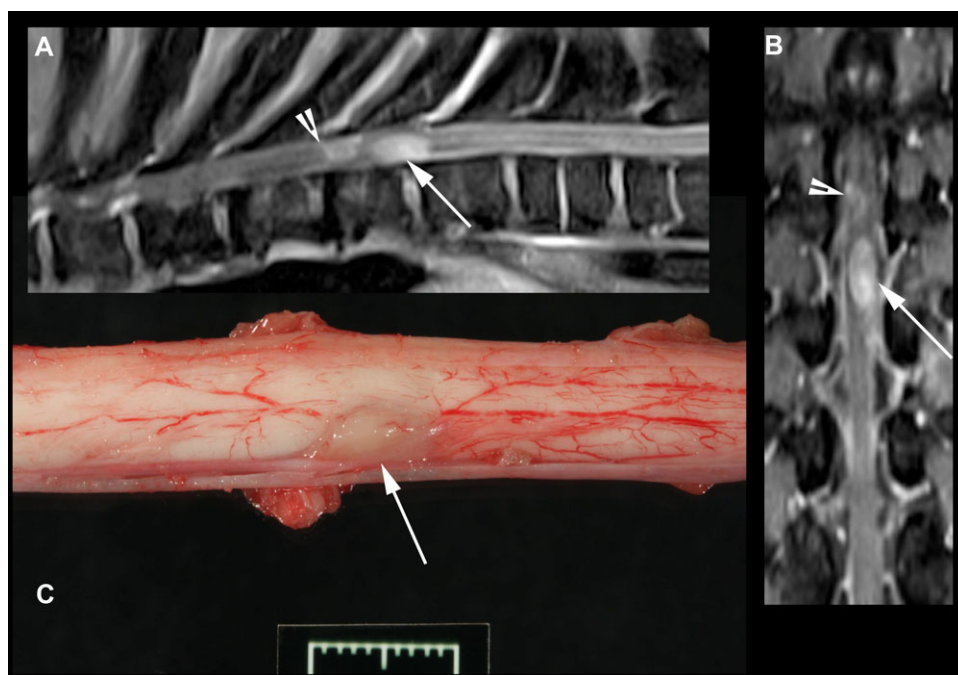


FIG. 2. (A) Sagittal T1-weighted image with chemical fat suppression postcontrast (TR 625.0 ms, TE 11.0 ms, and 3.0 mm). (B) Dorsal T1-weighted image with chemical fat suppression postcontrast (TR 825.0 ms, TE 11.0 ms, and 2.0 mm). (C) Gross image demonstrating the tan, glistening mass visible on the left dorsal aspect of the spinal cord at the level of the T9 vertebra. The arrowhead denotes the right-sided mass and the arrow denotes the left-sided mass. The marker in the gross image is 1.0 cm.

On T1-weighted sequences the lesions were isointense to mildly hyperintense compared to the spinal cord white matter (Fig. 1B). On postcontrast images, the mass lesions uniformly and strongly contrast enhanced with marked peripheral enhancement (Fig. 1A). In addition, there was a central region of increased enhancement in the caudal mass lesion. There was generalized meningeal enhancement within the imaging field of view, that extended to T6 cranially and T12 caudally (Fig. 1A, 2A, 2B). At the level of T9, the peripheral margin of the spinal cord parenchyma and dura were irregular and T2 hyperintense, with thickening and enhancement of the dura. This finding is suggestive of a dural

tail sign. The masses had imaging characteristics of both intramedullary and intradural extramedullary disease processes. A neoplastic process was considered the most likely diagnosis with primary consideration given to metastatic neoplasia, lymphoma, glial cell tumor, meningioma, and other round cell neoplasms. Due to the meningeal enhancement and multifocal lesions, granulomatous disease was also considered.

Based on the MRI findings of multifocal spinal cord mass lesions, a poor prognosis of recovering neurologic function was concluded. Euthanasia was elected and a necropsy was performed. An intradural, $5 \times 3 \times 3$ mm,

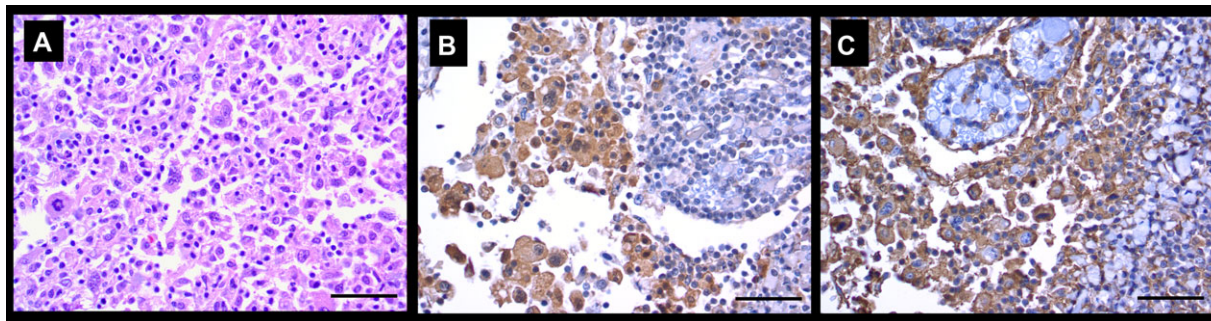


FIG. 3. (A) Histopathologic image of the neoplasm, demonstrating the following features of the neoplastic round cells: moderate to abundant cytoplasm, marked anisocytosis and anisokaryosis, multinucleation, erythrophagocytosis, and occasional bizarre mitotic figures [Hematoxylin and eosin, 400 \times magnification]. Immunohistochemistry for CD11d (B) and CD18 (C) shows strong, diffuse staining of the neoplastic cells with both antibodies, supporting a histiocytic origin [400 \times magnification]. Calibration mark within each image is 50 microns.

soft, tan, glistening mass was identified in the spinal cord at the level of the T9 vertebra (Fig. 2C). The mass was located on the left dorsal aspect of the spinal cord and extended into the parenchyma. On cut section, a second similar intramedullary mass was identified just cranial to the first. Histologic examination revealed a densely cellular, relatively well-demarcated, infiltrative neoplasm, which occupied approximately two-thirds of the spinal cord area and markedly compressed the neighboring parenchyma. The neoplasm was composed of dense sheets of round cells supported by a fine fibrovascular stroma. Neoplastic cells had distinct cytoplasmic borders, a moderate to large amount of eosinophilic cytoplasm, and irregularly oval to reniform nuclei with coarsely stippled chromatin and one to two small nucleoli. Anisocytosis and anisokaryosis were marked, and multinucleated cells were common. The mitotic rate was approximately one mitosis per 40 \times field with occasional bizarre mitoses (Fig. 3A). A few neoplastic cells contained intracytoplasmic erythrocytes (erythrophagocytosis). Infiltrating the neoplasm were large numbers of lymphocytes and plasma cells, which often formed thick cuffs around vessels. The neoplastic and inflammatory cells extended into the leptomeninges and invaded spinal nerve roots, but did not extend extradurally. The neoplastic cells were immunopositive for CD18, CD11d, Iba1, and CD45RA, supporting a histiocytic origin (Fig. 3B and C). The cells were negative for S100, cytokeratin, CD3, and CD79a. The histologic appearance and immunohistochemical profile of the neoplastic cells led to a diagnosis of histiocytic sarcoma.

Discussion

Histiocytes are a category of leukocytes that have an integral role in immune system function and occur in many tissues throughout the body.¹ Histiocytes are derived from stem cell precursors and differentiate into cells of the monocyte/macrophage lineage or dendritic cell lineage.¹ The histiocytic disorders can be classified into the canine cutaneous

histiocytoma, histiocytic sarcoma complex, and reactive histiocytoses.²⁻⁷ The histiocytic sarcoma complex includes both localized and disseminated histiocytic sarcoma^{1,2,8} with the malignant cells demonstrating histiocytic morphologic and immunophenotypic features.⁹ Histiocytic sarcomas may be localized to a single organ with solitary or multiple lesions, and are capable of rapid and widespread metastasis.⁶ Histiocytic sarcoma is frequently observed in Bernese mountain dogs, Rottweilers, Golden Retrievers, Flat-coated Retrievers, and Labrador Retrievers.^{1,2,4,6-8,10} Organs commonly affected by malignant histiocytic sarcoma include the spleen, liver, lymph nodes, bone marrow, lung, and skeletal muscle.^{2,4-8,10,11}

In dogs, disseminated histiocytic sarcoma affecting multiple organs, including the central nervous system (CNS), is well described in the literature. Focal and diffuse histiocytic sarcoma confined to and only involving the CNS is uncommon with limited publications in dogs and humans.^{3,5-11} Two case reports of spinal cord histiocytic sarcoma have been published previously with imaging findings discussed in one of the reports.^{7,11} The MR imaging in the previous report characterized the neoplastic lesion as diffuse parenchymal disease, involving the spinal cord and meninges.⁷ Unlike the previously reported spinal cord histiocytic sarcoma⁷, discrete mass lesions with diffuse meningeal enhancement were seen in this case. This variation to the imaging appearance of spinal histiocytic sarcoma, with multifocal mass lesions, is similar to what has been previously described in the brain of dogs.⁵⁻⁸ To the author's knowledge, this is the first imaging description for this form of histiocytic sarcoma in the spinal cord of a dog.

Meningeal enhancement and focal mass lesions are also seen in lymphoma¹² with anaplastic large cell lymphoma being the most important differential diagnosis for histiocytic sarcoma in humans.⁹ Furthermore, the imaging findings of dural tail sign, with dural enhancement and dural thickening, are observed with meningioma.¹³ However, the dural tail sign is not specific for meningioma and can be seen with other tumors including histiocytic sarcoma

and lymphoma.^{5,12,13} The imaging findings of meningeal enhancement and focal dural thickening support the previous report of dural tail sign associated with histiocytic sarcoma in the brain⁵ and reinforce the fact that dural tail sign is not specific for meningioma in dogs.^{5,13}

The imaging characteristics in this particular case made it difficult to determine the specific anatomic location of the lesion. An intradural location was suspected, however due to the overlapping imaging characteristics including medullary mass lesions, meningeal enhancement and dural tail sign, intradural extramedullary and intramedullary lesions were considered in the differential diagnosis. This is a common limitation and has been previously noted when evaluating the imaging-based characterization of both canine and human spinal cord neoplasia.^{14,15}

Histiocytic sarcoma is a rare neoplasm of the spinal cord with imaging characteristics that overlap other spinal cord

neoplasms, including meningioma and lymphoma^{5,7,9,12} and without its own distinguishing appearance. It has been difficult to establish diagnostic criteria for histiocytic sarcoma in dogs due to the variability in clinical presentation and imaging characteristics.^{5,7,11} Current veterinary research directed toward the identification of histopathologic markers to substratify histiocytic disorders is an important step in this process.^{1,2,9} A definitive histologic diagnosis is essential prior to the initiation of therapy, as the imaging characteristics of histiocytic sarcoma can resemble other neoplasms that vary with respect to recommended treatment and prognosis.^{1,5,7-9,12} Because of the similarity of imaging characteristics to other neoplastic lesions, histiocytic sarcoma should be considered in dogs with clinical signs of T3-L3 myelopathy when multifocal contrast enhancing mass lesions with dural tail sign and meningeal enhancement are seen on MR imaging.

REFERENCES

1. Fulmer A, Mauldin G. Canine histiocytic neoplasia: an overview. *Can Vet J* 2007;48:1041–1050.
2. Moore P, Affolter V, Vernau W. Canine hemophagocytic histiocytic sarcoma: a proliferative disorder of CD11d+ macrophages. *Vet Pathol* 2006;43:632–645.
3. Ide T, Uchida K, Kagawa Y, Suzuki K, Nakayama H. Pathological and immunohistochemical features of subdural histiocytic sarcomas in 15 dogs. *J Vet Diagn Invest* 2011;23:127–132.
4. Schultz R, Puchalski S, Kent M, Moore P. Skeletal lesions of histiocytic sarcoma in nineteen dogs. *Vet Radiol Ultrasound* 2007;48:539–543.
5. Tamura S, Tamura Y, Nakamoto Y, Ozawa T, Uchida K. MR imaging of histiocytic sarcoma of the canine brain. *Vet Radiol Ultrasound* 2009;50:178–181.
6. Thio T, Hilbe M, Grest P, Pospischil A. Malignant histiocytosis of the brain in three dogs. *J Comp Path* 2006;134:241–244.
7. Tzipory L, Vernau K, Sturges B, et al. Antemortem diagnosis of localized central nervous system histiocytic sarcoma in 2 dogs. *J Vet Intern Med* 2009;23:369–374.
8. Affolter V, Moore P. Localized and disseminated histiocytic sarcoma of dendritic cell origin in dogs. *Vet Pathol* 2002;39:74–83.
9. Sun W, Nordberg M, Fowler M. Histiocytic sarcoma involving the central nervous system. *Am J Surg Pathol* 2003;27:258–265.
10. Chandra A, Ginn P. Primary malignant histiocytosis of the brain in a dog. *J Comp Path* 1999;121:77–82.
11. Uchida K, Morozumi M, Yamaguchi R, Tateyama S. Diffuse leptomeningeal malignant histiocytosis in the brain and spinal cord of a Tibetan terrier. *Vet Pathol* 2001;38:219–222.
12. Palus V, Volk H, Lamb C, Targett M, Cherubini G. MRI features of CNS lymphoma in dogs and cats. *Vet Radiol Ultrasound* 2012;53:44–49.
13. Graham J, Newell S, Voges A, Roberts G, Harrison J. The dural tail sign in the diagnosis of meningiomas. *Vet Radiol Ultrasound* 1998;39:297–302.
14. Abul-Kasim K, Thurnher M, McKeever P, Sundgren P. Intradural spinal tumors: current classification and MRI features. *Neuroradiology* 2008;50:301–314.
15. Kippenes H, Gavin P, Bagley R, Silver G, Tucker R, Sande R. Magnetic resonance imaging features of tumors of the spine and spinal cord in dogs. *Vet Radiol Ultrasound* 1999;40:627–633.